# Inter–Injection–Locked Oscillators with Applications to Spatial Power Combining and Phased Arrays

*Karl. D. Stephan*
*Department of Electrical and Computer Engineering*
*University of Massachusetts*
*Amherst, MA 01003*

Summary

Although the principle of injection locking has been applied to single– and multiple–device oscillators at microwave through millimeter wavelengths, the technique has not found many uses in hybrid or monolithic microwave integrated circuits. We present here a novel circuit topology which leads to the inter–injection–locking of a set of interconnected oscillators. Since each oscillator is coupled only to its two nearest neighbors, the scheme is very well adapted to integrated planar construction. Furthermore, phase control of only one injection power source can control the phases of all oscillators in the system in a manner suitable for driving a phased antenna array. A summary of the theory is followed by a description of results from an experimental VHF three–oscillator system. We conclude with a discussion of some proposed applications of inter–injection–locked systems.

## Single Injection–Locked Oscillator

The most complete treatment of microwave oscillators injection–locked to an external source is contained in a series of works by Kurokawa [1,2,3]. He based his work on what we shall term a canonical oscillator circuit in which the active device is simplified to a nonlinear impedance whose real part is allowed to be negative. Unlike Kurokawa's single–cavity multiple–device analysis, however, we begin by assuming that each device is embedded in its own oscillator circuit, forming a complete unit which may be coupled to other units in a controlled fashion. Planar circuit technology makes this assumption viable under most circumstances. Except for this difference, our analysis of a single–device oscillator is merely a dual form of Kurokawa's treatment.

The canonical oscillator (Fig. 1) contains an active nonlinear element $Y_D(A) = -G_D(A) + jB_D(A)$ whose real and imaginary components depend in a nonlinear way upon the peak amplitude A of the presumably sinusoidal voltage across its terminals. In parallel with the active element $Y_D(A)$ is an equivalent tank circuit having inductance $L$ and capacitance $C$, as well as an equivalent load conductance $G_L$.

The injection signal $i(t)$ in Fig. 1 is a current which, by Kirchoff's current law, is the sum of the currents through the various components:

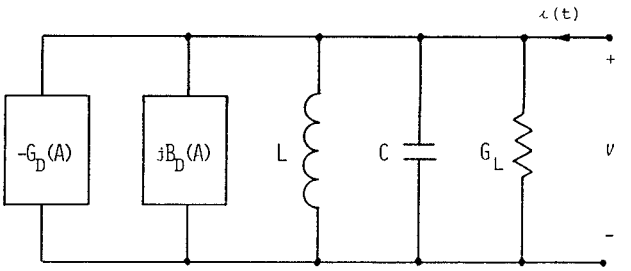


Fig. 1. Canonical oscillator circuit.

$$C\frac{dv}{dt} + G_L v + \frac{1}{L}\int v\,dt + Y_D v = i(t) \tag{1}$$

We now make an important assumption about the nature of the voltage $v$. Let

$$v = A(t)\cos[\omega_i t + \phi(t)] \tag{2}$$

where the peak voltage amplitude $A(t)$ and the instantaneous phase $\phi(t)$ are both slowly varying functions of time. The phase is measured with respect to an arbitrary reference frequency $\omega_i$, and the modifier "slowly" refers to the rate of change with respect to one period of the reference frequency. The assumption of slowly varying amplitude and phase allows us to neglect higher–order terms arising when equation (2) is inserted into equation (1). Integration by parts yields the following expression:

$$\begin{aligned} &C\{-A[\omega_i + \frac{d\phi}{dt}]\sin(\omega_i t + \phi) + \frac{dA}{dt}\cos(\omega_i t + \phi)\} \\ &\quad + (G_L - G_D)[A\cos(\omega_i t + \phi)] - B_D A\sin(\omega_i t + \phi) \\ &\quad + \frac{1}{L}\{(\frac{A}{\omega_i} - \frac{A}{\omega_i^2}\ \frac{d\phi}{dt})\sin(\omega_i t + \phi) \\ &\quad + \frac{1}{\omega_i^2}\frac{dA}{dt}\cos(\omega_i t + \phi)\} = i \end{aligned} \tag{3}$$

At this point we make an assumption about the injected current $i(t)$. We assume that it consists of a cosinusoidal in–phase component of magnitude $I_c(t)$ in phase with the oscillator, plus a quadrature sinusoidal component of magnitude $I_s(t)$:



0149-645X/86/0000-0159$01.00 © 1986 IEEE

$$i(t) = I_c(t)\cos(\omega_i t + \phi) + I_s(t)\sin(\omega_i t + \phi) \qquad (4)$$

Substitution of (4) into (3) allows us to multiply both sides of the expression by $\sin(\omega_i t + \phi)$ and integrate over one cycle. Orthogonality eliminates the cosine terms and leaves:

$$\frac{d\phi}{dt}(C + \frac{1}{\omega_i^2 L}) + B_D + \omega_i C - \frac{1}{\omega_i L} = -\frac{I_s}{A} \qquad (5)$$

When (3) is multiplied by $\cos(\omega_i t + \phi)$ and integrated, we have

$$\frac{dA}{dt}(C + \frac{1}{\omega_i^2 L}) + (G_L - G_D)A = I_c \qquad (6)$$

For radian injection frequencies $\omega_i$ near the free-running oscillator frequency $\omega_o = 1/\sqrt{LC}$, we define a frequency deviation $\Delta\omega = \omega_i - \omega_o$ so that

$$C + \frac{1}{\omega_i^2 L} \approx 2C \qquad (7)$$

$$\omega_i C - \frac{1}{\omega_i L} \approx 2\Delta\omega C \qquad (8)$$

We thus arrive at differential equations in time for the amplitude and phase of the oscillator voltage:

$$\frac{d\phi}{dt} = -\Delta\omega - \frac{B_D}{2C} - \frac{I_s}{2CA} \qquad (9)$$

$$\frac{dA}{dt} = \frac{A}{2C}(G_D - G_L) + \frac{I_c}{2C} \qquad (10)$$

In the absence of injection current ($I_c = I_s = 0$), equation (10) shows that the steady-state amplitude $A_o$ is reached when $G_D(A) - G_L = 0$, making $dA/dt = 0$. It is also clear that the in-phase component $I_c$ of the injection current has a first-order effect on amplitude, while instantaneous frequency ($= d\phi/dt$) is primarily influenced by the quadrature component $I_s$.

## Coupled Oscillators

The derivations leading to equations (5) and (6) above allow us to embed one or more canonical oscillators in a linear circuit of our choosing. Given an initial amplitude $A(t)$ and phase $\phi(t)$ for each oscillator, linear circuit theory leads to a solution for the injection current $i(t)$ which can be resolved into components $I_c$ and $I_s$ for each oscillator. Equations (9) and (10) can then be numerically integrated for $A(t)$ and $\phi(t)$, leading to a time-domain solution of the system.

It is evident that the behavior of such a system depends critically on the characterization of the oscillators in terms of negative conductance $-G_D(A)$ and susceptance $B_D(A)$. Although in principle these functions can be obtained from a nonlinear circuit analysis program such as SPICE, it is probable that more reliable data is obtained from direct load-pull measurements. In these measurements, an external variable admittance $Y_{ext}$ is connected to the injection node of an actual oscillator. Frequency and power variations resuling from $Y_{ext}$ variations are translated into the functions $-G_D(A)$ and $B_D(A)$. In many cases, the variation of device susceptance $B_D(A)$ can be neglected, and this was done in the results to be presented, although improved accuracy can be obtained by including $B_D(A)$.

A computer program was written to predict the behavior of three identical oscillators (Fig. 1) embedded in the linear circuit of Fig. 2. The oscillator characteristics $L$, $C$, and $G_D(A)$ were obtained from load-pull measurements and are described below. With no injection current, it was found that for virtually any set of realistic initial conditions, the oscillator phases gravitated toward each other by virtue of the currents through coupling conductances $G_C$. When in-phase injection currents were introduced, the three-oscillator system sychronized to the injection frequency much as a single oscillator would.

A most interesting phenomenon occurred when the phase of one injection signal was shifted with respect to the other ($\psi_3 \neq \psi_0$). As shown in Fig. 3, the phases of the oscillators spread out in equally-spaced intervals proportional to the injection phase difference $\psi_3 - \psi_0$. The

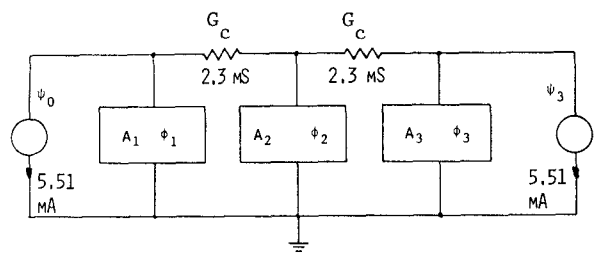


Fig. 2. Three canonical oscillators of Fig. 1 in inter-injection-locked cascade.

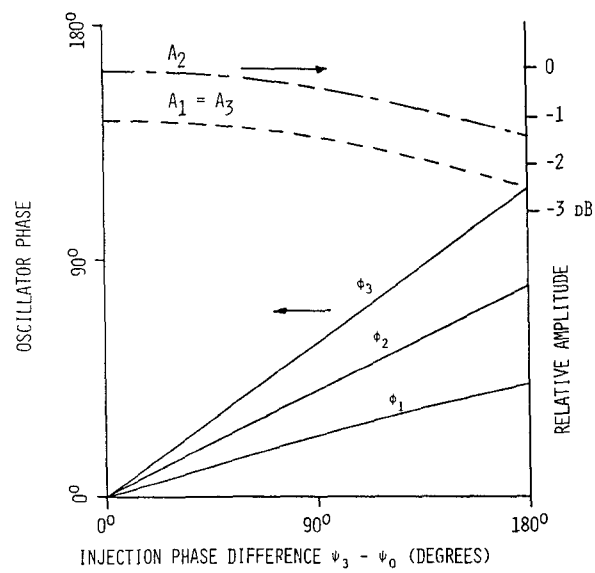


Fig. 3. Predicted amplitudes and phases of Fig. 2 oscillators versus injection phase difference $\psi_3 - \psi_0$.

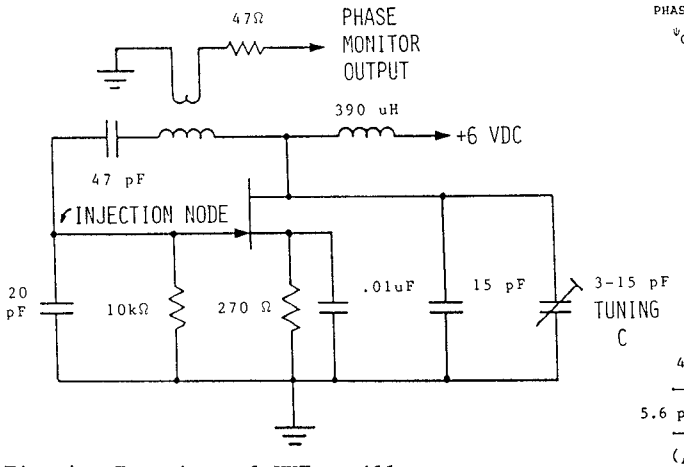


Fig. 4. Experimental VHF oscillator.

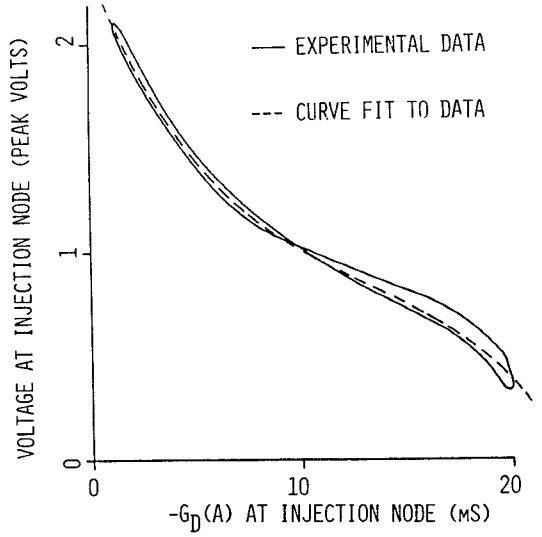


Fig. 5. $-G_D(A)$ of Fig. 4 oscillator.

predicted oscillator phases are linear with respect to the injection phase difference to within ±4%, and the predicted amplitude variations are relatively minor. This linear phase progression from one source to the next is precisely the behavior required to drive a steerable linear phased antenna array, and in the simulation the control of all three oscillator phases was achieved by controlling the phase of only one injection power source.

## Experiments

A three–oscillator system was designed to emulate the computer simulation at 220.3 MHz. Each oscillator used a VHF JFET in the circuit of Fig. 4. Load–pull experiments led to a functional dependence of $-G_D(A)$ shown in Fig. 5, and modeled by the mathematical single–valued interpolation shown by the dashed line. Due to a slight dependence of $G_D$ on frequency, the experimental curve is a narrow closed loop rather than a single–valued line, but

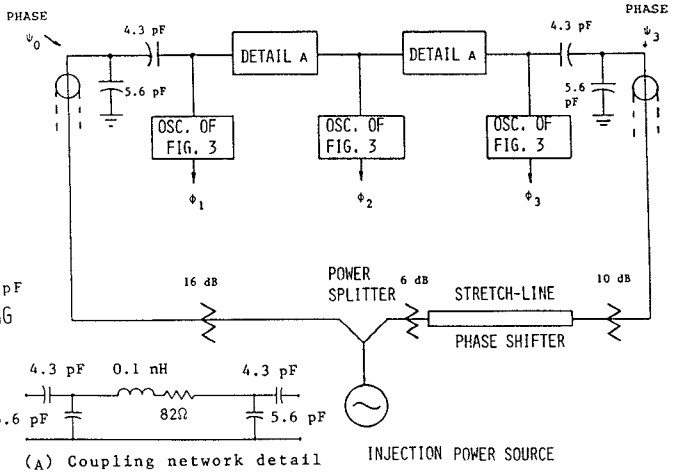


Fig. 6. Test setup for three-oscillator inter-injection-locking experiment.

this slight dependence was neglected. A value of $C = 212$pf was determined for the equivalent capacitance of the Fig. 1 circuit, and an equivalent inductance $L = 2.46$nH resonates the tank circuit at 220.3 MHz.

Since the actual oscillators are housed in separate shielded enclosures, it was not possible to use a simple resistor to interconnect injection nodes. Instead, coupling capacitances were included in coupling circuits shown in Fig. 6(A), which were designed to have the same mutual Y–parameter as the desired coupling conductance $G_C$. (Shunt admittances can be absorbed in the oscillator equivalent circuits.) Unfortunately, the design neglected certain stray reactances and resulted in an equivalent coupling admittance closer to $Y_c = 1.55 - j0.42$mS. Additionally, the simulation's injection current value of 5.51 mA was found to be outside the range of applicability of the oscillator model. Accordingly, a new computer simulation was run with the experimentally measured complex value of $Y_C$ and smaller injection currents of 1.74 mA. The predicted phase behavior of this system is shown in Fig. 7. The undesirable curvature of the phase lines is caused by the reactive part of the coupling admittance.

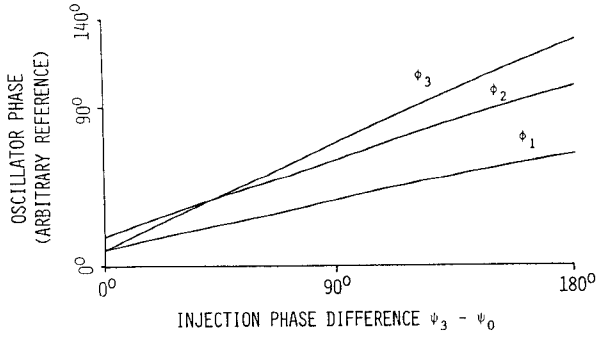


Fig. 7. Predicted oscillator phases of Fig. 6 versus injection phase difference $\psi_3 - \psi_0$ using revised values of $Y_c$ and injection current.

In the test setup of Fig. 6, the injection phases $\psi_0$ and $\psi_3$ were equalized by means of the stretch–line phase shifter. The oscillator tuning adjustments were set so as to equalize the oscillator phases to $\pm 10^\circ$ or so. Then, the injection phase difference $\psi_3 - \psi_0$ was increased and the oscillator phases were measured as shown in Fig. 8. Agreement with the theoretical prediction of Fig. 7 is reasonably good, and can no doubt be improved with more detailed models of the oscillators.

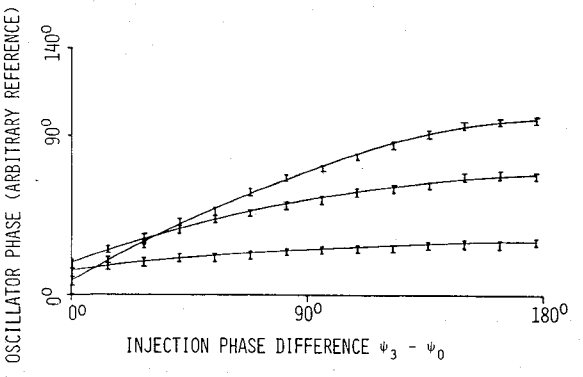


Fig. 8. Measured oscillator phases of Fig. 6 versus injection phase difference $\psi_3 - \psi_0$.

## Applications

The applications of inter–injection–locked arrays fall into two categories: (a) *All-in-phase applications*, in which no phase control other than keeping the oscillators in phase with each other is required, and (b) *Phased array applications*, for which a linear progression of phase shift per oscillator is controlled by a single external phase shifter.

The number of inter–injection–locked oscillators that can be used in a given situation depends upon each oscillator's frequency accuracy and external Q. External Q [4] is a measure of how easily an oscillator is pulled by a given level of injection power. An ideal oscillator for use in an inter–injection–locked array would have a free–running frequency exactly equal to the injection frequency, and a low value of external Q so that its phase may easily be controlled by a small amount of injection power. Real oscillators do not meet these ideal specifications, but computer simulations using statistical distributions of frequency errors indicate that systems using four to eight oscillators should be feasible without post–production tuning.

Fig. 9 shows a phased antenna array which could be used for either in–phase spatial power combining or steerable phased–array applications. Beneath each patch antenna is an active device which uses the patch as a resonant element. Coupling between patches can be adjusted to provide the desired inter–injection–locking behavior, and radiation from each antenna into free space combines at a distant point without losses. Much effort is required for the characterizaton of self and mutual impedances of such a system, but progress in this area is being made [5]. This basic principle is applicable from microwave frequencies on

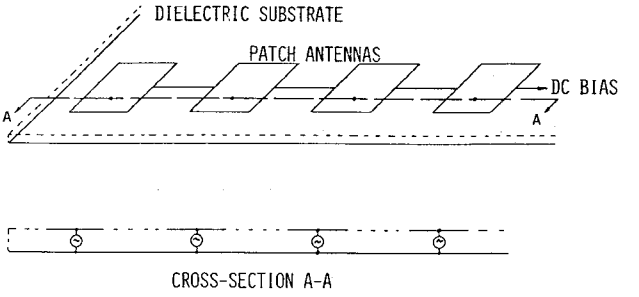


Fig. 9. Proposed inter–injection–locked phased array of microstrip antennas driven by active devices.

through the millimeter–wave range [6], where the very limited power available from an individual device makes low–loss power combining a desirable option.

## Conclusions

The principle of inter–injection–locked oscillators has been analyzed and experimentally verified in a three–oscillator system. Although close frequency tolerances may be necessary for large systems, the concept should be applicable to many planar and monolithic circuits in which the total power requirement exceeds that available from one device.

## References


1. K. Kurokawa, "Noise in Synchronized Oscillators," **IEEE Trans. Microwave Theory Tech.**, Vol. MTT–16, pp. 234–240, Apr. 1968.
2. K. Kurokawa, "Some Basic Characteristics of Broadband Negative Resistance Oscillators," **Bell System Tech. Jour.**, Vol. 48, pp. 1937–1955, July–Aug. 1969.
3. K. Kurokawa, "The Single–Cavity Multiple–Device Oscillator," **IEEE Trans. Microwave Theory Tech.**, Vol. MTT–19, pp. 793–801, Oct. 1971.
4. K. Kurokawa, *An Introduction to the Theory of Microwave Circuits*, (New York: Academic Press, 1969), p. 388.
5. D.M. Pozar, "Input Impedance and Mutual Coupling of Rectangular Microstrip Antennas," **IEEE Trans. Antennas and Prop.**, Vol. AP–30, pp. 1191—1196, Nov. 1982.
6. J.W. Mink, "Quasi–Optical Power Combining of Solid–State Millmeter–wave Sources," **IEEE Trans. Microwave Theory Tech.**, Vol. MTT–34, pp. 273—279, Feb. 1986.